文章编号：0258-7025(2009)03-0558-06

Comparative investigation on amplifying performance between 980 nm and 1480 nm pumped bismuth-based EDFA

Yaxun Zhou(周亚训)*, Na Gai(盖 娜), Fen Chen(陈 芬), and Gaobo Yang(杨高波)

(*College of Information Science and Engineering, Ningbo University, Ningbo, Zhejiang* 315211, *China*)

* *Corresponding auther: zhouyaxun@nbu.edu.cn*

Received October 19, 2008; revised January 4, 2009

Abstract The population rate and power propagation equations are presented and solved to compare the amplification performances of bismuth-based Er^{3+}-doped fiber amplifier (EDFA) pumped by 980- and 1480-nm lasers, respectively. In both single signal and coarse wavelength-division-multiplexing (CWDM) signals inputs, the 1480-nm pumped bismuth-based EDFA provides a larger signal gain than the 980-nm pumped one does, whereas the latter provides a relatively lower noise figure (NF). Comparative results indicate that the 1480-nm pumping scheme is more advantageous for bismuth-based EDFA regarding the band width and gain property.

Key words optical communications; amplification performances; rate equations; power propagation equations; bismuth-based EDFA

CLCN: TN929.11 **Document Code**: A **doi**: 10.3788/CJL20093603.0558

1 Introduction

With the exponential increases of information capacity in optical networks, Er^{3+}-doped fiber amplifiers (EDFAs) applied for wavelength-division-multiplexing (WDM) systems have been extensively developed. Since silica-based transmission fiber has a wide low-loss window from 1.4 to 1.7 μm, amplification in this whole range is required for broadband WDM systems. Of which C-band amplification from 1.53 to 1.56 μm is firstly accomplished by using the silica-based EDFA [1, 2]. In order to extend C-band to a broader wavelength range, Er^{3+}-doped fibers made of non-silicate glass hosts with high refractive indices such as tellurite-[3] and bismuth-based [4] glasses are developed because the stimulated-emission cross sections increase as the refractive indices of the hosts increase $[\sigma \sim (n^2+2)^2/n]$ [5], and as a result they become possible to obtain amplification gain in a broader wavelength range than silica-based host with low refractive index. However, tellurite-based EDFs cannot be fusion-spliced to silica-based transmission fiber because its softening temperature is much lower than that of silica-based glass. Recently, amplification over 75-nm bandwidth of 3-dB down gain (1535～1610 nm) covering from C- to L-band with signal gain over 19 dB has been demonstrated by using fusion-spliceable bismuth-based EDFs [6], indicating that bismuth-based EDFs can be the prospective candidates for (C + L)-band broad applications regarding the gain and fusion-splice properties.

To amplify the 1.5-μm band signal, conventional EDFAs use optical pumping of 980 or 1480 nm in accordance with the energy levels of Er^{3+}. Pumping at 1480 nm is typically used for high power EDFAs because the ground state absorption to the $^4I_{13/2}$ manifold has a high absorption cross section relative to the $^4I_{11/2}$ energy level. Unfortunately, this resonant pumping scheme cannot achieve full population inversion and a good value of signal-to-noise ratio [7]. Thus, to realize a fiber amplifier of a lower noise figure (NF) along with a broadband gain, a 980-nm pumping scheme may be essential. In spite of the advantages of bismuth-based glass as a host material and its Er^{3+}-doped fiber already having been pointed out [4], comparative results for bismuth-based EDFA under the 980- and 1480-nm excitation, which are essential to optimize amplifier performances, are not available so far.

In this paper, we present the population rate and light power propagating equation models of bismuth-based EDFA, and make a comparative investigation on the amplification performances between the 980- and 1480-nm pumping schemes numerically. The difference in the amplification performances is understood by comparing the NF, the dependence of signal gain on the input power, and the fiber length.

This work was financially supported by the Natural Science Foundation of Zhejiang Province (Y107070), the Natural Science Foundation of Ningbo City (2006A610026), and was sponsored by K. C. Wong Magna Fund in Ningbo University

2 Theory

The schematic diagram of energy levels together with the proposed transitions of Er^{3+} is shown in Fig. 1. The transitions are indicated with an arrow and represented from left to right for different cases: 980-nm excitation, spontaneous radiation and nonradiative decays, absorption and stimulated emission at 1.5 μm, 1480-nm excitation, and finally the upconversion process. N_1, N_2, N_3, and N_4 represent the populations of the energy levels $^4I_{15/2}$, $^4I_{13/2}$, $^4I_{11/2}$, and $^4S_{3/2}$, respectively. For the sake of simplicity, we neglect the intermediate levels between the $^4I_{11/2}$ and $^4S_{3/2}$ levels and assume that all the Er^{3+} ions excited to the $^4F_{7/2}$ level via the pump excited state absorption (ESA) transit nonradiatively to the $^4S_{3/2}$ level, and all the Er^{3+} ions excited to the $^4I_{9/2}$ level by the upconversion process relax to the $^4I_{11/2}$ level immediately[8], since no significant peaks corresponding to radiative transitions from these levels are detected in the emission measurement for bismuth-based glass.

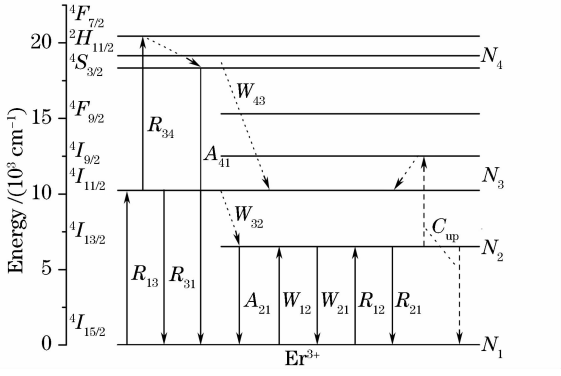

Fig. 1 Energy level diagram of Er^{3+} and the relevant transitions. R_{13}, R_{31}, and R_{34} are for the 980-nm pump only. Corresponding, R_{12} and R_{21} are for the 1480 nm only

The amplification characteristics of the bismuth-based EDFA can be investigated by theoretical analyses. The power propagations of the signal, pump and amplified spontaneous emission (ASE) along the Er^{3+}-doped fiber are described by the following differential equations[8, 9]:

$$
\begin{aligned}
&\frac{\mathrm{d}P_s}{\mathrm{d}z} = 2\pi P_s \int_0^{r_{Er}} [\sigma_s^e N_2 - \sigma_s^a N_1]\psi_s \, r\mathrm{d}r - \alpha_s P_s ,\\
&\frac{\mathrm{d}P_{p\pm}}{\mathrm{d}z} = \pm 2\pi P_{p\pm} \int_0^{r_{Er}} [\sigma_p^e N_2 - \sigma_p^a N_1]\psi_p \, r\mathrm{d}r \mp \alpha_p P_{P\pm}, \text{ (for 1480-nm pumping)}\\
&\frac{dP_{p\pm}}{dz} = \pm 2\pi P_{p\pm} \int_0^{r_{Er}} [\sigma_p^e N_3 - \sigma_p^a N_1 - \sigma_{ESA}^a N_3]\psi_p \, r\mathrm{d}r \mp \alpha_p P_{P\pm}, \text{ (for 980-nm pumping)}\\
&\frac{dP_{ASE\pm}}{dz} = \pm 2\pi P_{ASE\pm} \int_0^{r_{Er}} [\sigma_{ASE}^e N_2 - \sigma_{ASE}^a N_1]\psi_{ASE} \, r\mathrm{d}r \pm 2\pi h\upsilon_{ASE}\Delta\upsilon_{ASE} \int_0^{r_{Er}} \sigma_{ASE}^e N_2 \psi_{ASE} \, r\mathrm{d}r \mp \alpha_{ASE} P_{ASE\pm},
\end{aligned}
\tag{1}
$$

where P is the light power, the subscripts s, p, and ASE represent the signal, pump, and ASE [forward (+) and backward (−) propagation], respectively. ψ is the normalized power mode field profile, α is the fiber background loss, σ^a and σ^e are the absorption and emission cross sections at the signal, pump, and ASE wavelengths, respectively. Here, we apply the Quimby's assumption that the ESA absorption cross section σ_{ESA}^a is equal to $2\sigma_p^a$[10]. In the ASE equation, $\Delta\upsilon_{ASE}$ represents the effective ASE bandwidth, h is the Plank's constant, and r_{Er} is the fiber Er^{3+}-doped radius. The populations N_1, N_2, N_3, and N_4 of Er^{3+} can be obtained by solving the following steady-state rate equations pumped at the 980 and 1480 nm, respectively.

2.1 1480-nm pump

Under the 1480-nm excitation, the level scheme introduced in Fig. 1 leads to the following population rate equations of Er^{3+}:

$$
\begin{aligned}
\frac{\mathrm{d}N_1}{\mathrm{d}t} &= -(W_{12}+R_{12})N_1 + (R_{21}+A_{21}+W_{21})N_2 + C_{up}N_2^2 ,\\
\frac{\mathrm{d}N_2}{\mathrm{d}t} &= (W_{12}+R_{12})N_1 - (R_{21}+A_{21}+W_{21})N_2 + W_{32}N_3 - 2C_{up}N_2^2 ,\\
\frac{\mathrm{d}N_3}{\mathrm{d}t} &= -W_{32}N_3 + C_{up}N_2^2 ,\\
N_1 + N_2 + N_3 &= N_T ,
\end{aligned}
\tag{2}
$$

where N_T is the Er^{3+}-doped concentration in the glass. A_{21} is the spontaneous emission transition rate from the $^4I_{13/2}$ to $^4I_{15/2}$ level, W_{32} is the nonradiative decay rate from the $^4I_{11/2}$ to $^4I_{13/2}$ level, and C_{up} is the homogeneous upconversion energy transfer coefficient for the process of $^4I_{13/2} + {}^4I_{13/2} \rightarrow {}^4I_{9/2} + {}^4I_{15/2}$. Here, we neglect the nonradiative decay rate of the $^4I_{13/2}$ level and the spontaneous emission

from the $^4I_{11/2}$ level because A_{21} and W_{32} are dominant in those levels. The ESA for pumping at 1480 nm is also negligible because this wavelength does not match with the transition from the $^4I_{13/2}$ to $^4I_{9/2}$ level [11]. $W_{12/21}$ and $R_{12/21}$ are the absorption- and emission-stimulated rates at the 1.5-μm band signal and 1480-nm pump wavelengths, respectively, and can be defined as [12,13]

$$W_{12/21} = \sum_{i=1}^{M} \frac{\sigma^{a/e}(\upsilon_s^i)}{h\upsilon_s^i} P_s^i \psi_s^i + \sum_{j=1}^{N} \frac{\sigma^{a/e}(\upsilon_{ASE}^j)}{h\upsilon_{ASE}^j} [P_{ASE+}^j + P_{ASE-}^j] \psi_{ASE}^j,$$

$$R_{12/21} = \frac{\sigma^{a/e}(\upsilon_p)}{h\upsilon_p} [P_{p+} + P_{p-}] \psi_p, \quad (3)$$

where M is the number of propagating signals, N is the number of frequency slots with bandwidth $\Delta\upsilon_{ASE}$ centered at the frequency υ_{ASE} to represent the ASE noise spectrum [14].

2.2 980-nm pump

As shown in Fig. 1, the rate equations of Er^{3+} under the 980-nm excitation can be described as

$$\frac{dN_1}{dt} = -(R_{13} + W_{12})N_1 + (A_{21} + W_{21})N_2 + C_{up}N_2^2 + R_{31}N_3 + A_{41}N_4,$$

$$\frac{dN_2}{dt} = W_{12}N_1 - (A_{21} + W_{21})N_2 - 2C_{up}N_2^2 + W_{32}N_3,$$

$$\frac{dN_3}{dt} = R_{13}N_1 + C_{up}N_2^2 - (W_{32} + R_{31} + R_{34})N_3 + W_{43}N_4,$$

$$\frac{dN_4}{dt} = R_{34}N_3 - A_{41}N_4 - W_{43}N_4,$$

$$N_1 + N_2 + N_3 + N_4 = N_T, \quad (4)$$

where R_{13} and R_{31} are the transition rates of 980-nm pump stimulated absorption and emission, respectively, R_{34} is the ESA rate from the $^4I_{11/2}$ to $^4F_{7/2}$ level, which can be defined as the similar form of Eq. (3). A_{41} is the spontaneous emission rate from the $^4S_{3/2}$ to $^4I_{15/2}$ level, and W_{43} is the nonradiative decay rate from the $^4S_{3/2}$ to $^4I_{11/2}$ level. The rest parameters used in Eq. (4) are the same as those in Eq. (2).

Equations (1)～(4) form a system of coupled differential equations, which can be solved by the numerical integration along the fiber using the fourth-order Runge-Kutta algorithm with appropriate boundary conditions:

$$P_{p+}(0) = P_{p0}, \quad P_{p-}(L) = P_{pL}$$
$$P_s(0,\upsilon_s^i) = P_{s0}(\upsilon_s^i), \quad (i = 1, M)$$
$$P_{ASE+}(0,\upsilon_{ASE}^j) = P_{ASE-}(L,\upsilon_{ASE}^j) = 0, \quad (j = 1, N) \quad (5)$$

where L is the active fiber length of bismuth-based EDFA.

The two-boundary value problem formed by Eq. (1) cannot be solved simultaneously. Therefore, an iterative scheme may be used. Initially, the co-propagation pump, M signals, and the N ASE+ equations are integrated in the forward direction, doing $P_{p-}(z) = 0$ and $P_{ASE-}(z,\upsilon^j) = 0\ \forall\ z$. Then, the counter-propagation pump and the N ASE− equations are integrated in the backward direction, using the power distribution obtained in the forward direction as their input conditions. This iterative procedure, forward followed by the backward integration, is repeated until that convergence takes place. The parameters used for numerical calculations are listed in Table 1. The absorption and emission cross sections of Er^{3+} in the 1520～1620 nm region are determined from the measured absorption spectrum of bismuth-based glass fabricated with conventional melting and annealing method.

Table 1 Parameters used for numerical calculations[8, 9, 15]

Parameter	Value
Spontaneous emission rate A_{21}/s^{-1}	330
Spontaneous emission rate A_{41}/s^{-1}	2800
Non-radiative decay rate W_{32}/s^{-1}	7500
Non-radiative decay rate W_{43}/s^{-1}	75000
Cooperative upconversion coefficient $C_{up}/(m^3/s)$	8.5×10^{-24}
Emission cross section at 1480-nm σ_p^e/cm^2	1.19×10^{-21}
Emission cross section at 980-nm σ_p^e/cm^2	3.06×10^{-21}
Absorption cross section at 1480-nm σ_p^a/cm^2	3.61×10^{-21}
Absorption cross section at 980-nm σ_p^a/cm^2	2.36×10^{-21}
Background loss α /(dB/m)	0.6
ASE effective bandwidth $\Delta\upsilon$ /nm	2.0×10^{-9}
Er^{3+} doped concentration N_T/cm^{-3}	7.51×10^{19}
Er^{3+} doped radius $r_{Er}/\mu m$	2.5
Fiber core refractive index n	2.039
Numerical aperture NA	0.20

3 Numerical results and discussion

Figure 2 shows the signal gain spectra simulated by the single-wavelength operation for a bismuth-based EDFA pumped at 1480 and 980 nm, respectively. The bismuth-based EDFA with 150-cm fiber length is pumped bidirectionally with a pump power of 360 mW (forward 180 mW and backward 180 mW). The input signal wavelength is scanned from 1520 to 1620 nm and each signal power is changed in steps: −20, −10, and 0 dBm, respectively. As can be observed, the gain spectra of both 1480- and 980-nm pumped bismuth-based EDFA exhibit broadband profiles even in an extended L-band region to 1620 nm. This result reflects the excel-

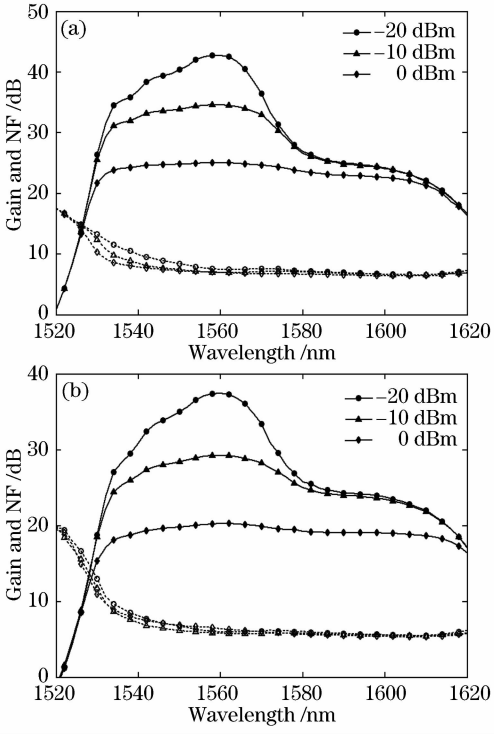

Fig. 2　Gain and NF with input signal power for bismuth-based EDFA pumped at 1480 nm (a) and 980 nm (b), respectively

lent broad spectroscopic properties of Er^{3+} in bismuth-based glass [4]. However, under the same operating conditions described above, it is easily envisaged that the much larger signal gains are obtained in the 1480-nm pumped bismuth-based EDFA than the 980-nm pumped one across the whole spectral range, which implies that the 1480-nm pumping scheme is advantageous for achieving high signal gain and output power bismuth-based EDFA. In this pumping scheme, maximum gain exceeds 40 dB and the gain at 1560 nm is about 6.3 dB larger than that of the 980-nm pumping at the input signal power of −20 dBm. The lower signal gain in the 980-nm pumped bismuth-based EDFA is attributed mainly to the ESA of ${}^4I_{11/2} \rightarrow {}^4F_{7/2}$, which decreases the pump conversion efficiency (PCE). With the increase of the input signal power, signal gains in the range of about 1532～1578 nm are compressed because of the gain saturation. At the saturated condition of the input signal power of 0 dBm, flat amplification with bandwidth of 76 nm, signal gain over 22 dB, and a gain excursion of less than 3 dB in the 1530～1606 nm range covering from C- to L-band are obtained in the 1480-nm pumping. While in the 980-nm pumping case, the corresponding 3-dB down bandwidth is increased to 83 nm (1533～1616 nm) with the gain over 17 dB, which means that the latter pumping scheme can offer a flatter gain spectrum. Meanwhile, Fig. 2 also presents the NF (dotted line). Both the 980- and 1480-nm pumped bismuth-based EDFA exhibit a low NF profile even beyond the wavelength of 1610 nm. Compared to the 1480-nm pumping, the NF in the 980-nm pumped bismuth-based EDFA is relatively lower except the short wavelength region near 1520 nm, in which an obvious increasing NF is observed due to the decrease of signal gain. At the input signal power of 0 dBm, the minimum 5.3 dB of NF is obtained. This result contrasts with the minimum 6.4 dB of NF for 1480-nm pumped EDFA.

Figure 3 shows the effect of fiber length on the signal gain and NF pumped bidirectionally at 1480 and 980 nm, respectively. The pump power is kept at 360 mW (forward 180 mW and backward 180 mW), the input signal power is set to 0 dBm, and the fiber length is changed in steps: 60, 150, and 250 cm. It is clear that the bismuth-based EDFA can amplify signals sufficiently in both C- and L-band with single signal operation using short length of fiber. With the increase of the fiber length, there is a dramatic decrease of signal gain in the short wavelength region and an obvious increase in the long wavelength region around 1600 nm, with the amplifying gain band changing from C- to L-band still keeping the higher signal gain, lower NF,

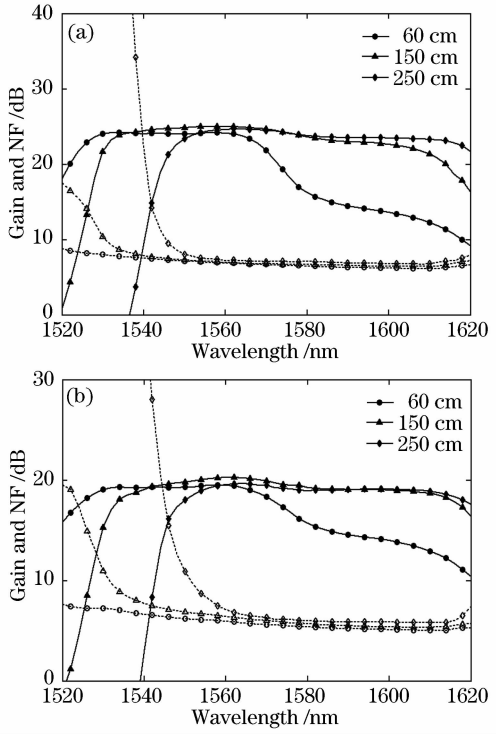

Fig. 3　Gain and NF with fiber length for bismuth-based EDFA pumped at 1480 nm (a) and 980 nm (b), respectively

and broader flat amplification at any fibers. Under the 1480-nm excitation, for example, the bandwidth of 3-dB down gain is 47 nm (1523～1570 nm) for 60-cm fiber, 76 nm (1530～1606 nm) for 150-cm fiber, and 73 nm (1546～1619 cm) for 250-cm fiber, while the corresponding 55-nm (1521～1576 nm), 83-nm (1533～1616 nm), and 73-nm (1547～1620 cm) bandwidth of 3-dB down, respectively, are found in the 980-nm pumped bismuth-based EDFA. This indicates that for a bismuth-based EDF selecting a shorter length (～60 cm) is suitable for C-band amplifiers, a longer one (～250 cm) for extended L-band amplifiers, and an immediate one (～150 cm) for (C + L)-band amplifier for both 1480- and 980-nm pumping. The gain band change from C- to extended L-band is mainly due to the radiation trapping effect that transfers energy from short wavelengths to long wavelengths [16], which enhances with fiber length as a result of the increasing interaction distance of photons. The radiation trapping is often occurred in a three-level system where the absorption and emission spectra overlap. Besides, when the fiber length is relatively short, for example, 60 cm, the NF is kept low in the entire wavelength range of 1520～1620 nm, and the minimum of NF is 5.0 dB in the 980-nm pumped bismuth-based EDFA, while 6.1 dB in the 1480-nm pumped one. With the increase of fiber length, the NF increases slightly for both pumping schemes. This is attributed to the gradually accumulation process of ASE along the fiber.

Figure 4 shows the signal gain and NF for four-channel coarse WDM (CWDM) signals pumped at 1480 and 980 nm, respectively. The total input power of four CWDM signals with 20-nm channel spacing and wavelength ranging from 1556 to 1616 nm is 0 dBm (－6.02 dBm × 4 signals). The pump power is the same as before (forward 180 mW and backward 180 mW) and the fiber length of bismuth-based EDF is 2.0 m. It is seen again that the 1480-nm pumped bismuth-based EDFA has a larger gain than the 980-nm pumped one for each channel. Corresponding to the 1480- and 980-nm pumping cases, more than 19- and 14-dB gain per channel can be obtained for CWDM signals spreading the 60 nm bandwidth, respectively. Whereas the NF is relatively low in the latter except for the short wavelength channel. The best and worst NFs among the four channels are 4.4 dB and 6.4 dB, while 4.9 and 5.6 dB in the 1480-nm pumped one. Relatively flat ASE output indicates that the bismuth-based EDFA has a tolerance for the fluctuation of signal wavelength. At present, CWDM system is emerging as a mainstream technology for metro access optical networks due to its low cost and design simplicity. However, applying commercial silica-based EDFA for the CWDM amplifier that has more than four-channels is difficult because of it relatively narrower bandwidth. For example, PureGain5500 amplifier by Avanex has 20.5 dB of single-channel gain only in the C-band (1530-1562 nm) or in the L-band (1570-1605 nm) region, and such amplifier which includes the channel of 1610 nm has not been reported. Here, the bismuth-based EDFA exhibits high performance with broadband and low NF in both single signal and CWDM signals applications.

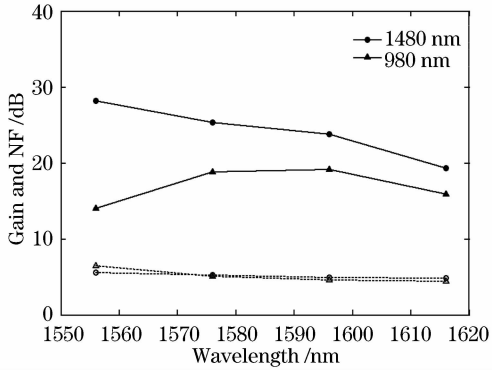

Fig. 4 Gain and NF for four CWDM signals of bismuth-based EDFA pumped at 1480 nm and 980 nm, respectively

4 Conclusions

The amplifying performances of bismuth-based EDFA pumped at 1480 and 980 nm have been compared. It is shown theoretically that the 1480-nm pumped EDFA can provide larger signal gain in both single signal and CWDM signals uses, whereas the 980-nm pumped EDFA can provide relatively low NF. The simulation results clearly indicate that the 1480-nm pumping scheme is more suitable for achieving high gain and power EDFA, while the 980-nm pumping scheme is suitable for low NF EDFA. Therefore, a hybrid pumping scheme which combines 1480- and 980-nm lasers may be essential to achieve a broadband bismuth-based EDFA with both high gain and low NF.

References

1 R. Mears, L. Reekie, I. M. Jauncey *et al*.. Low-noise erbium-doped fiber amplifier operating at 1.54 μm [J]. *Electron. Lett.*, 1987, **23**(19): 1026～1028

2 E. Desurvire, J. R. Simpson, B. C. Becker. High-gain erbium-doped traveling-wave fiber amplifier [J]. *Opt. Lett.*, 1987, **12**(11): 888～890

3 Zhou Yaxun, Wang Jun, Dai Shixun *et al*.. Effect of Yb^{3+} on infrared and upconversion emission of Er^{3+} doped tellurite-based glasses[J]. *Chinese J. Lasers*, 2007, **34**(12): 1688～1693

周亚训，王　俊，戴世勋 等. Yb^{3+}对掺铒碲酸盐玻璃红外和上转换发光的影响[J]. 中国激光，2007，**34**(12)：1688～1693

4 S. Tanabe, N. Sugimoto, S. Ito *et al*.. Broad-band 1.5 μm emission of Er^{3+} ions bismuth-based oxide glasses for potential WDM amplifier[J]. *J. Lumin.*, 2000, **87～89**: 670～672

5 J. S. Wang, E. M. Vogel, E. Snitzer. Tellurite glass: a new candiate for fiber devices[J]. *Opt. Mater.*, 1994, **3**(3): 187～203

6 S. Ohara, N. Sugimoto, K. Ochiai *et al*.. Ultra-wideband amplifiers based on Bi_2O_3-EDFAs [J]. *Opt. Technol.*, 2004, **10**(4): 283～295

7 W. J. Miniscalco. Erbium-doped glasses for fiber amplifiers at 1500 nm [J]. *J. Lightwave Technol.*, 1991, **9**(2): 234～250

8 H. Hayashi, S. Tanabe, N. Sugimoto. Quantitative analysis of optical power budget of bismuth oxide-based erbium-doped fiber [J]. *J. Lumin.*, 2008, **128**(3): 333～340

9 H. Hayashi, N. Sugimoto, S. Tanabe. High-performance and wideband amplifier using bismuth-oxide-based EDF with cascade configurations [J]. *Opt. Fiber Technol.*, 2006, **12**(3): 282～287

10 R. S. Quimby. Output saturation in a 980-nm pumped erbium-doped fiber amplifier[J]. *Appl. Opt.*, 1991, **30**(18): 2546～2552

11 Y. Hu, S. Jiang, G. Sorbello *et al*.. Numerical analyses of the population dynamics and determination of the upconversion coefficients in a new high erbium-doped tellurite glass[J]. *J. Opt. Soc. Am. B*, 2001, **18**(12): 1928～1934

12 A. P. Lopez-Barbero, W. A. Arellano-Espinoza, H. L. Fragnito *et al*.. Tellurite-based optical fiber amplifier analysis using the finite-element method[J]. *Microwave Opt. Technol. Lett.*, 2000, **25**(2): 103～107

13 Wu Yuexiang, Ma Xiaoming, Zhao Xiaoji. Effects of Er^{3+} and Yb^{3+} concentration on gain and noise coefficient of fiber amplifier [J]. *Acta Optica Sinica*, 2008, **28**(6): 1057～1061
吴粤湘，马晓明，赵晓吉. 铒镱共掺特性对光放大器增益和噪声系数的影响[J]. 光学学报，2008，**28**(6)：1057～1061

14 C. R. Giles, E. Desurvire. Propagation of signal and noise in concatenated erbium-doped amplifiers[J]. *J. Lightwave Technol.*, 1991, **9**(2): 147～154

15 H. Hayashi, N. Sugimoto, S. Tanabe *et al*.. Effect of hydroxyl groups on erbium-doped bismuth-oxide-based glasses for fiber amplifiers[J]. *J. Appl. Phys.*, 2006, **99**(9): 093105-1～093105-8

16 S. Dai, T. Xu, Q. Nie *et al*.. Investigation of concentration quenching in Er^{3+}:Bi_2O_3-B_2O_3-SiO_2 glasses[J]. *Phys. Lett. A*, 2006, **359**(4): 330～333